

THE ROLE OF SIMULATION IN EVALUATING THE BEHAVIOUR OF AN ELASTIC COUPLING WITH FLEXIBLE METALLIC ELEMENTS

Abstract: The paper presents the analysis of the elastic coupling with flexible elements, taking into consideration the mechanical strength criterion in conditions of normal loading or torsion overload, with and without misalignment, using finite element analysis, responding to multiple demands that are required in coupling structure. There are presented the basic principles for applying the finite elements method: the study of convergence at different mesh sizes, the loading scheme and boundary conditions for the flexible element. Also, the paper presents several simulations to prove the behaviour and functionality of the coupling for different operational scenarios: mechanical stress, buckling stability and modal analysis.

Key words: elastic coupling, flexible disc, stress state, finite element method (FEM), buckling stability.

INTRODUCTION

Considering the conventional methods of calculating the elastic couplings with metallic intermediate elements that introduce simplifying assumptions, it is necessary and appropriate to apply the finite element method to the design of these couplings. The Finite Element Method is an efficient calculation method that can be used in the current state of development of dimensional design and optimization of flexible elements, such as those in the elastic coupling structure with metallic membranes. The method also leads to cost and design time reduction, thus constituting a method of optimizing coupling design [1].

Finite element analysis is an integral part of structural analysis. For finite element analysis, the following steps must be taken: description of specific elements (element type, geometric constants, material); description of loads and boundary conditions; automatic generation of the finite element network; post - processing of results.

Conceiving the finite elements, i.e. establishing their shape, specifying the number of nodes in which they are interconnected, and the nature of these links must be made in such a way as to ensure that the structure can be reconstituted as accurately as possible.

The constructive solution adopted for the elastic coupling must be tested for its quality by theoretical simulations and practical experiments. Through simulation, an image of the behaviour and properties of the coupling is obtained before it can be manufactured and effectively used.

2. SIMULATION AND EVALUATION OF STRESS AND STRAIN STATE

2.1 Convergence study

The dimensions of the finite elements and their number were chosen in such a way as to approximate as closely as possible the actual continuous structure, from the point of view of the geometrical shape, the way of applying the loads, the boundary conditions, the stiffness, and the masses.

The set of boundary conditions must prevent the structure model from having rigid body movements or mechanism movements [5].

For modeling the model supports correctly and to avoid sources of errors in this modeling approach, the operating conditions of the flexible membrane and boundary conditions must be well known to best illustrate these situations.

The efficiency of the finite element model depends on the quality of the meshing process.

The meshed structure approximates geometrically and mechanically the actual structure.

The approximation is better, the results more precise and the volume of information obtained higher, the higher the number of nodes, respectively the total number of degrees of geometric freedom of the structure.

When developing the model, it was taken into account that the convergence process can be achieved in two ways:

- The use of "higher order" elements, which have polynomials of approximation as high as possible. This implies that the finite element has a larger number of nodes, with more degrees of geometric freedom and a more complicated geometric shape. From a computational point of view, this type of element is more efficient because it processes a larger amount of information;
- Making a finer meshing, i.e. the model has as many nodes and finite elements as possible (fig. 1).

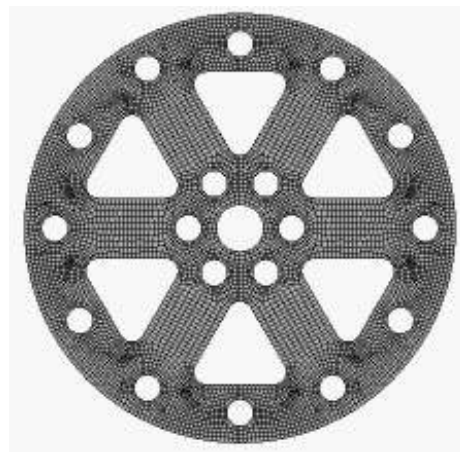


Fig. 1 Meshing of membrane with SHELL elements with four nodes[1].

The size and number of finite elements influence the convergence of the solution. Convergence to the exact solution was achieved by increasing the number of elements and modifying the type of finite element, even if the computational effort and implicitly the cost of the analysis increased when the number of elements increased. The results of the analysis, using four-node SHELL elements, are presented in table 1, which specifies the size of the finite element, numbers of nodes and number of elements, and the maximum equivalent stress and nodal displacements [1].

Table 1

The results of the analysis with SHELL element QUAD4

Side size [mm]	4	3	2	1	0.7	0.5
No. elements	471	845	1474	4724	6768	18677
No. nodes	603	1019	1752	5249	7494	19742
σ_{ech} [N/mm ²]	63.2	71.3	75.3	87.1	89.2	96.2
u_{sum} [μm]	15.9	16.9	17.2	17.6	17.6	17.7

In order to achieve convergence, it was taken into account that the model mesh network was as simple and uniform as possible. Switching from small items to large ones has been progressive.

In order to ensure an increase in model efficiency, it is preferable that a (moderate) increase in the number of nodes and model elements is accompanied by a non-uniform meshing, adapted to the configuration of the model's stress state.

It is necessary for the meshing to take into account the estimated configuration of the stress state of the structure and hence of the model, i.e. in areas with high gradients of the stress state the meshing is fine and in the other areas coarser.

Around the concentrators (holes, connecting areas) the sides of the finite elements have kept the dimensional ratio close to the unit, but at the same time these sides have diminished from those of the elements in the areas further away from the concentrator.

Considering the results with SHELL elements, with four nodes, in fig. 2 is illustrated, at increasingly fine meshing (i.e. having a greater number of nodes and elements), the convergence process of the solution.

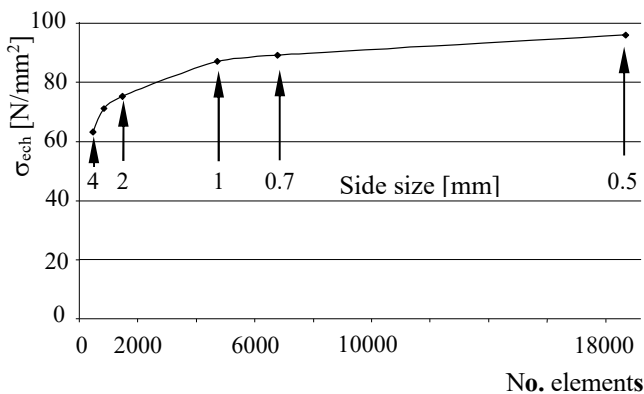


Fig. 2 Study of convergence at different mesh variants.

It is noted that to a larger number of elements, the result approaches the exact solution, although excessive growth leads to a large amount of calculations.

If 8-node SHELL elements are used, the meshed model contains 6395 elements, with 20655 nodes. The maximum equivalent stress, at a 5.4% meshing percentage error, is 95.8 N/mm².

Finer elements were used around the small holes and the short radius connections, and the location of the nodes was made in such a way as to ensure a uniformly spaced placement.

Considering this situation on the convergence level, the mesh with SHELL elements with 4 nodes, with the side dimension of 0.7 mm, was adopted, at which the value of the maximum equivalent stress, compared to the version with elements having the side of 0.5 mm, differs with less than 10%.

2.2 Description of the calculation model

The central problem to be solved when studying the flexible membrane by the finite element method is to establish the boundary conditions, so that the calculated characteristic corresponds, with some approximation, to the real characteristic determined experimentally. After determining the limit conditions, one can study the influence of the disc geometry on its elastic characteristic and the stress analysis can be performed.

For membrane study by FEM, finite elements of type SHELL were used. Due to geometric symmetry and load symmetry, only a 60° membrane sector can be studied.

For calculation was considered OLC 65A steel with the following mechanical characteristics (STAS 795-92):
 - the longitudinal elastic modulus $E = 2.06 \cdot 10^5$ N/mm²;
 - the cross-contractive coefficient $\mu = 0.33$;
 - admissible stress $\sigma_a = 320 \dots 420$ N/mm²;
 - $\sigma_r = 1000$ N/mm²; $\sigma_c = 800$ N/mm².

It is considered a blocked disk on the inner rivet layout circles and the tangential forces resulting from the application of torsional torque, acting at angular distances of 60°, on the screws circle, at the top of each spoke, in the connecting zone with the outer band of the membrane. The introduced restrictions therefore do not allow translations and rotations on the inner rivet arrangement circle.

The loading was introduced as uniformly distributed normal pressure acting on the semi-cylindrical surfaces of the radius $d_s/2$ in which are located the clamping screws of the elastic element with one of the semi-coupling in the direction of actuation of the driving torque (analysis performed with the ANSYS program, on the model meshed with SHELL elements, QUAD4).

The tangential force acting on each screw is expressed by the relationship:

$$\begin{aligned}
 F_{t1} &= \int_0^\pi p \sin \alpha \cdot r \, d\alpha \cdot h = \\
 &= p \cdot r \cdot h \cdot \int_0^\pi \sin \alpha \, d\alpha = \\
 &= prh (-\cos \alpha) \Big|_0^\pi = p \cdot d_s \cdot h
 \end{aligned}
 \tag{1}$$

where: h represents the thickness of the membrane; d_s - the diameter of the screw rod. Result:

$$p = \frac{F_{t1}}{d_s \cdot h} \quad (2)$$

The loading scheme and boundary conditions for the elastic element are shown in figure 3.

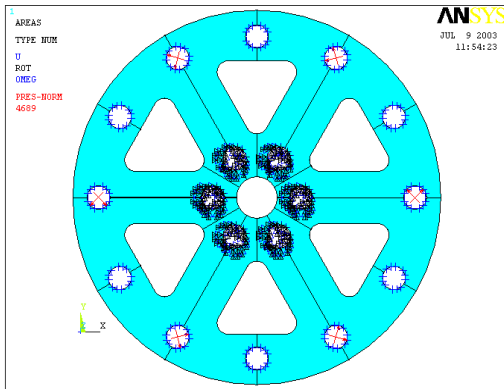


Fig. 3 Loading scheme of the elastic element.

In the nodes on the central part of the membrane, located on the outline of the inner holes, the displacements are null. All outer holes (including them serving for membranes packing) are blocked as displacement on the direction of the membrane axis. On the inner assembling holes, all the degrees of freedom (translation and rotation) are fixed in this portion.

2.3 Analysis of stress and strain state in the elastic membrane

The results of the meshing are shown in table 2.

Table 2

The results of the meshing of the structure		
Element type	No. elements	No. nodes
SHELL	6768	7494

For equivalent stresses, the results of the finite element analysis were presented in the form of different colored areas (color distribution), in fig. 4-6.

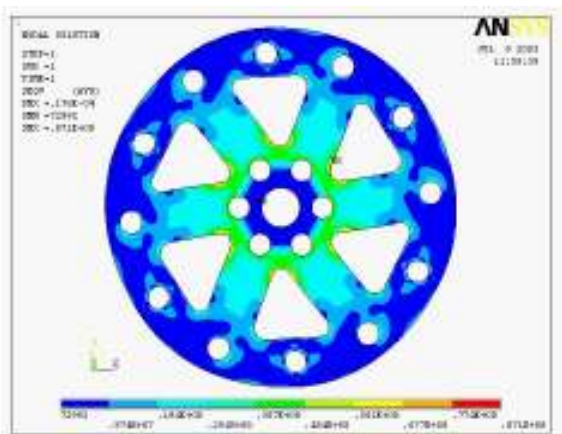


Fig. 4 Equivalent stress distribution, at $\Delta a = 0$, without considering centrifugal loading.

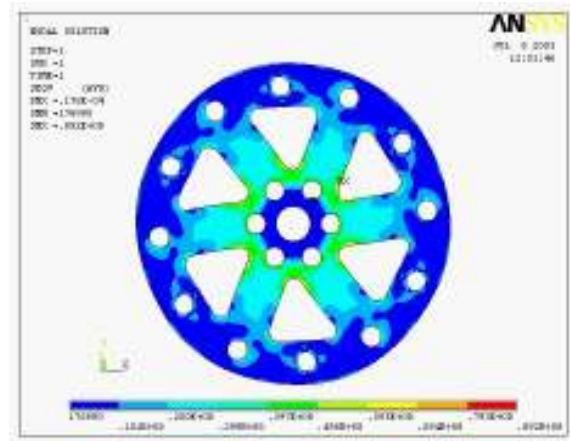


Fig. 5 Equivalent stress, taking into account the centrifugal loading, at $\Delta a = 0$.

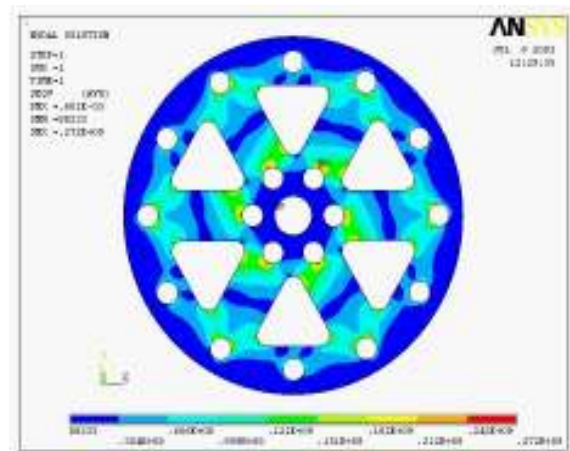


Fig. 6 Equivalent stress at axial deviation, $\Delta a = 0.6$ mm.

One would see that the maximum stress appears at the radius corresponding to filleted root of the spokes.

The maximum values of the equivalent stresses (calculated by the von Mises criterion) and the resulting displacement are shown in table 3.

Table 3

The values of the equivalent stresses and the resulting displacement, at $\Delta a = 0$			
Element type	Equivalent stress without centrifugal loading [N/mm ²]	Equivalent stress with centrifugal loading [N/mm ²]	Resulting displacement [μm]
SHELL	87.1	89.2	17.6

Centrifugal loading, due to the rotational speed ($n = 4500$ rpm), changes the maximum equivalent stress value from 87.1 N/mm² to 89.2 N/mm².

In figures 7 - 8 are shown the resulting deformation in the two situations: $\Delta a = 0$ and $\Delta a = 0.6$ mm.

Using the stress distribution of figures 5 and 6, it is possible to represent the variation diagram of the equivalent stress in relation to the radius of the spoke, in the direction of the spoke axis and its margin, for the two cases of presenting an axial deviation, as illustrated in figures 9 and 10.

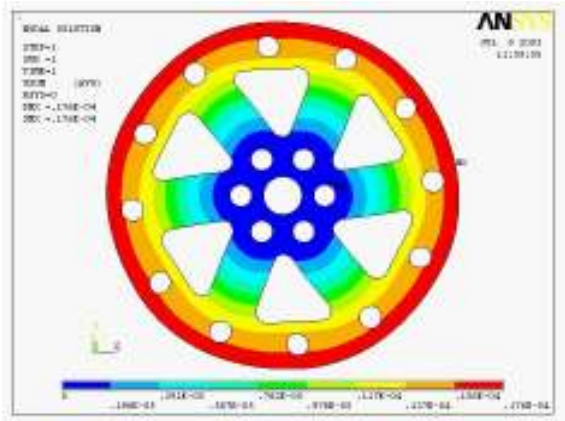


Fig. 7 Resulting displacement without axial misalignment.

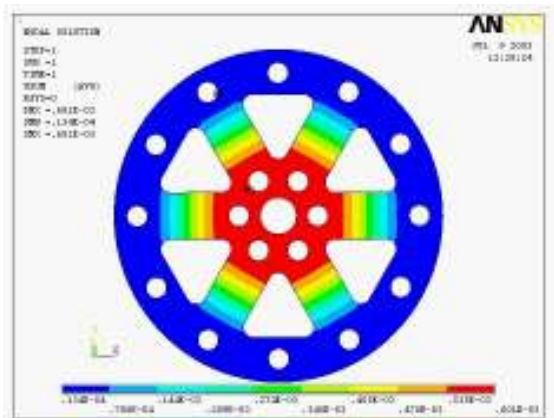


Fig. 8 Displacement with axial misalignment, $\Delta a = 0.6$ mm.

The graphs show that the equivalent stress reaches a maximum value on both the axis of the spoke and its edge at approximately equal radii, in the spoke connection zone with the center ring of the disc.

In the case of an axial misalignment $\Delta a = 0.6$ mm, the following values for stresses and deformations were obtained:

- resultant displacement $u_{rez\ ax} = 0.6002$ mm;
- the maximum stress at the base of the spokes $\sigma_{ech\ ax} = 272.3$ N/mm².

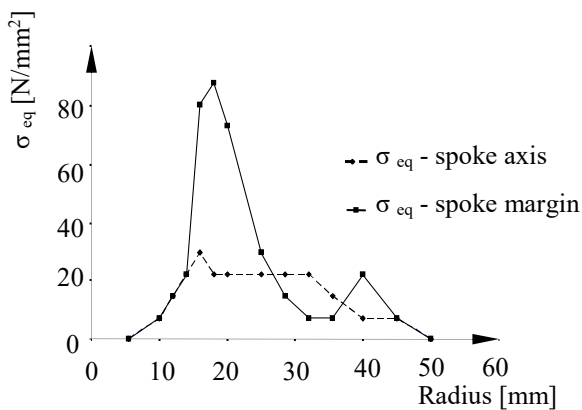


Fig. 9 Variation of the equivalent stresses versus the radius for the case $\Delta a = 0$.

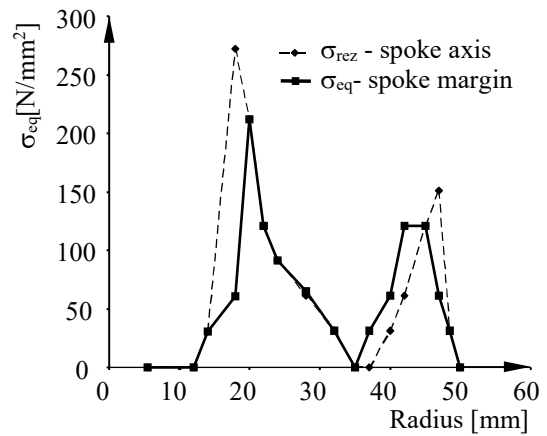


Fig. 10 Equivalent stresses versus the radius for 0.6 mm axial deviation.

2.4 Checking at stress sollicitation

The safety factor can be calculated with the general expression [1], [2]:

$$c = \frac{\sigma_{0.2}}{\sigma_{eq\ max}} \quad (4)$$

where $\sigma_{0.2}$ represent the yield point of the material. The steel used in calculus is OLC 65A, having $\sigma_{0.2} = 800$ N/mm². The admissible safety factor indicated in literature [3] for pieces subjected at fatigue is $c_a = 1.5...3$. The values of safety factor for the two cases of stress analysis and the discussion regarding the checking at stress sollicitation are shown in table 4.

Table 4
The values of safety factors in two situations:
 $\Delta a = 0$ and $\Delta a = 0.6$ mm

Size	Analysis case	
	$\Delta a = 0$	$\Delta a = 0.6$ mm
$\sigma_{eq\ max}$ [N/mm ²]	89.2	272
Safety factor, c	8.97	2.94
Checking discussion	$c > c_a$	$c \approx c_a$

The resulting strain and stresses σ_1 and σ_3 , as well as the equivalent stress for the two situations: without axial deviation ($\Delta a = 0$) and in the presence of axial deviation ($\Delta a = 0.6$ mm), are presented as values in table 5.

Table 5
Resulting strain and stress values

	u_{sum} [mm]	$\sigma_1\ max$ [N/mm ²]	$\sigma_3\ min$ [N/mm ²]	σ_{ech} [N/mm ²]
$\Delta a = 0$	0.0176	912	- 86.3	89.2
$\Delta a = 0.6$ mm	0.601	305	-	272

One would see that the introduction of axial misalignment ($\Delta a = 0.6$ mm) increases almost three times the principal stress σ_1 and the maximal equivalent stress given the situation without axial deviation.

3. SIMULATION OF TORSIONAL BUCKLING BEHAVIOUR

For linear (or eigenvalue) buckling analysis, the ANSYS program determines the scaling factors for the stress stiffness matrix. This formulation takes into account that the deflections are not large. The buckling load factor is generally a safety factor, defined as [1], [2]:

$$c = \frac{\text{Limit buckling load}}{\text{Applied load}} \quad (5)$$

The figure 11 illustrates the first buckling shape where the buckling load factor, c , is noted FREQ in the image of this figure.

The buckling load factors for 10 shape modes has values in the interval $c \in [9.455, 12.82]$, being greater than the ones admissible conforming to Niemann, $c_a = 3 \dots 5$. This demonstrates that the membrane is stable at buckling.

For a more comprehensive evaluation, the buckling analysis was made considering the influence of centrifugal loading due to the rotational speed, this situation determining a low increasing of the buckling safety factor with a percentage between 6% and 9%, by a specific stiffness effect [2]. With inertial loading, the values of buckling load factors are in the interval $c \in [10.329, 13.71]$.

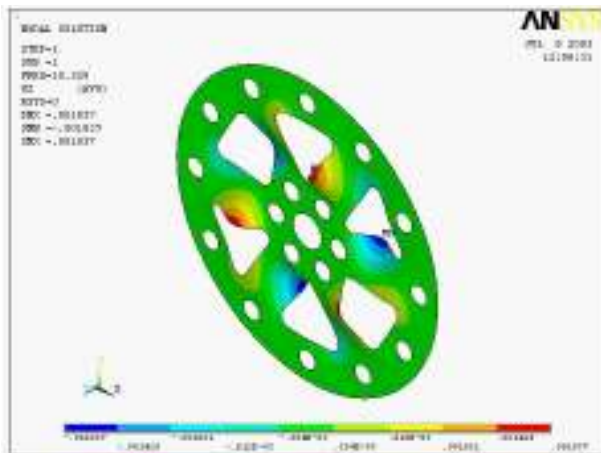


Fig. 11 First buckling shape for the case $\Delta a = 0$.

4. SIMULATION OF TORSIONAL VIBRATION BEHAVIOUR

Torsional vibration behaviour was simulated by FEM using SHELL type elements with 4 nodes. For calculation was considered the following parameters taken from specialized literature: torque of 50 N·m, rotation speed of 4500 rpm, thickness $h=0.3$ mm, modulus of elasticity $E=2.06 \cdot 10^5$ N/mm², density $\rho=7800$ kg/m³, Poisson's coefficient $\nu=0.33$ and shear modulus $G=8 \cdot 10^4$ N/mm².

The values obtained by modal analysis did not take into account inertial discontinuities. The proper frequencies and the corresponding modes shape vibrations have been determined for two cases of modal

analysis: without blockages on the outer holes and with restrictions on these holes (all the nodes are blocked so that the degree of freedom of rotation and translation are eliminated). The proper frequencies for these two cases of modal analysis are indicated in table 6 [1], [4].

The natural frequencies for 10 vibration modes have values in the interval $f \in [2067, 2556]$. This means that the membrane is stable at vibrations.

In the figures 12-15 are shown only three modes shape vibrations for these two situations.

Table 6

Results obtained by modal analysis		
Vibration mode	Without blockages on the outer holes	With blockages on the outer holes
1	157.5	2067
2	157.5	2087
3	157.6	2087
4	198	2139
5	198	2139
6	308	2176
7	373	2534.5
8	575	2541
9	575	2541
10	879	2556

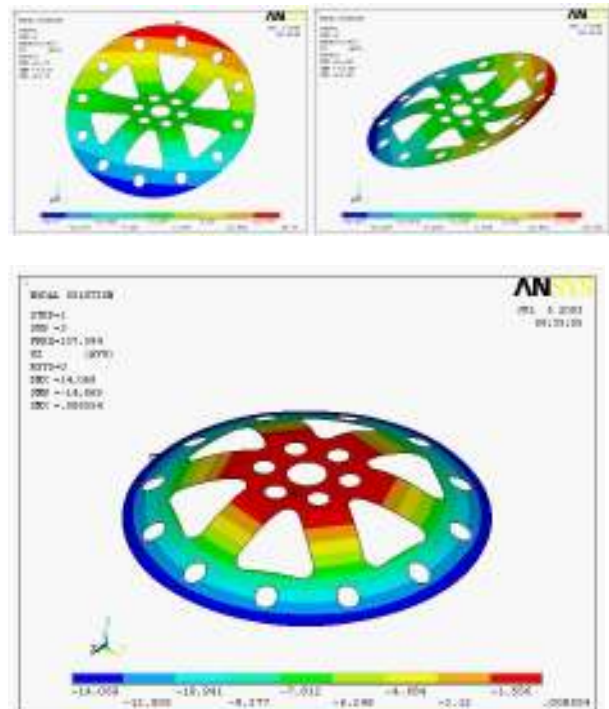


Fig. 12 The first three modal shapes of vibrations without blockages on the outer holes.

Due to symmetry, the first and second modes have similar shapes, which were obtained at approximately the same frequency, vibrations taking place around two perpendicular axes. The loading torque changes insignificantly their elastic membrane vibration frequencies [1], [4].

The input parameters of a membrane that are subject to change are geometric parameters such as fillet radius

or spokes' width but may be also loads locations or constraints location, thereby reducing dynamic solicitation and extending coupling life.

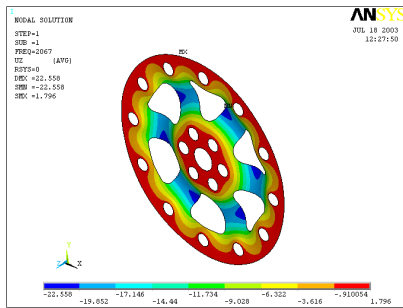


Fig. 13 The first modal shape of vibration with restrictions on the outer holes.

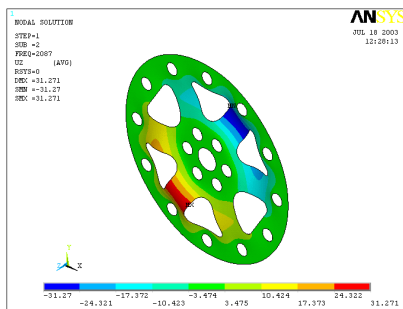


Fig. 14 The second modal shape of vibration.

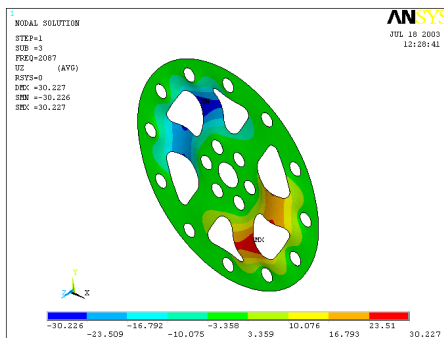


Fig. 15 The third modal shape of vibration.

The results of the evaluation are used to increase efficiency and feasibility of the membrane design.

5. CONCLUSIONS

In relation to the theoretical aspects, the following conclusions can be drawn:

- The conventional methods of calculating the elastic couplings with metallic intermediate elements are based on simplifying assumptions, so that it is necessary and appropriate to apply the finite element method to analyze the coupling structure;
- Finite element method (FEM) is the only calculation method that can be used in the current state of development of conceptual design and optimization of elastic elements from the structure of flexible membrane couplings; the method leads, in addition, to reducing costs and design time, thus constituting a method of optimizing coupling design;

- The calculation method used allows geometric changes to be made so that the influence of the geometry of the disc on its characteristics can be studied and the stress analysis can be obtained;
- The analysis of strain and stress state of the metallic disc is necessary to determine the maximum stress area in the disc spokes;
- The equivalent stress calculated with the von Mises criterion has the maximum value at the base of the spokes in their connection zones with the central portion of the membranes;
- Increase of the connection radii in these areas result in the decrease of the stresses of the concentrators, together with the widening of the loading area;
- Increasing the rotation speed of the disc also leads to the decrease of tensile and compression stresses due to the stiffening effect in the radial direction produced on the flexible membrane;
- The introduction of axial misalignments along the axis of the discs leads to significant stresses in the same areas, resulting in bending and tensile stresses due to the increase in the distance between the ends of the spokes; it is therefore necessary to introduce bending radii in the fastening areas for the parts with which the membranes are assembled.
- Product simulation certifies that the coupling works as expected. The simulation results should then be validated by practical experiments on closed or open power circuit stands to verify the compliance of the operating principle with the assumptions made in the analysis process.

REFERENCES

- [1] Dobre, D. (2004). *Researches on multi-criteria optimization of elastic couplings with metallic flexible membranes*, PhD Thesis, University Politehnica of Bucharest.
- [2] Dobre, D., Dobre, G., Mirică, R., Sorohan, S. (2003). *On strain and stress state of the metallic membranes at flexible coupling*, Proceedings of the International Conference "Power Transmissions '03", vol.1, ISBN 945-90272-9-5, pp. 69-72, Varna, Bulgaria.
- [3] Niemann, G. (1981). *Maschineelemente*, Springer Verlag, Berlin.
- [4] Dobre, D., Simion, I., Ioniță, E., Dobrescu, T. (2011). *Modal analysis of the metallic membrane from elastic coupling structure*, Annals of DAAAM for 2011 & Proceedings of the 22th International DAAAM Symposium, pp. 0319-0320, ISSN 1726-9679, ISBN 978-3-901509-73-5, Vienna, Austria.
- [5] Sorohan, S. & Sandu M.A. (1997). *Nonlinear FEM-Analysis of a Diaphragm Spring*, ELFIN 4, pp. 125-128, Constanta, Romania.

Author:

Associate prof. Daniel DOBRE, Ph.D., University Politehnica of Bucharest, Department of Engineering Graphics and Industrial Design, Romania. E-mail: ddobre@yahoo.com